# Investigation on the Interaction of Prulifloxacin with Human Serum Albumin: A Spectroscopic Analysis

Ya-Bei HUANG,[a,b] Shi-Jun WANG,[b] Yan-Qin ZI,*[,a] Zhang YU,[a] Xiao-Yan GAO,[a] Ying-Cai TANG,[a] and Da-Ming ZHANG[a]

[a] *Department of Chemistry, Huaibei Coal Normal College; No. 100 Dongshan Road, Huaibei, Anhui Province 235000, P. R. China: and* [b] *Huaibei Occupational Disease Prevention and Cure Hospital; No. 1 Xiangshan Road, Huaibei, Anhui Province 235000, P. R. China.*

Received December 5, 2009; accepted December 21, 2009; published online January 18, 2010

**The interaction between prulifloxacin (PUFX) and human serum albumin (HSA) was investigated under simulated physiologic conditions with fluorescence spectra. The fluorescence quenching process of HSA may be mainly governed by a static quenching mechanism. The apparent binding constant $K_b$ between PUFX and HSA at different temperatures were 2.08±1.04, 2.74±0.50, and 4.98±1.61×10$^8$ l/mol. The thermodynamic parameters, with a negative value of $\Delta G^0$, revealed that the binding is a spontaneous process. A binding distance $R$ of 1.19 nm between donor and acceptor was obtained from the Fŏrster energy transfer theory.**

**Key words** prulifloxacin; human serum albumin; fluorescence quenching; Stern–Volmer equation; thermal dynamic analysis

Proteins are important in living beings and take part in almost all life processes. They are not only involved in metabolism, immunity, and life evolution but also offer much information about ourselves. Human serum albumin (HSA), the most abundant protein in plasma, acts as a transporter and disposer of many endogenous and exogenous compounds.[1—3] HSA consists of a single polypeptide chain of 585 amino acid residues and comprises three structurally homologous domains: I (residues 1—195); II (196—383); and III (384—585). It comprises three contiguous domains, each containing two subdomains (A and B) that possess common structural motifs conferred by various intra- and interdomain forces such as salt bridges and hydrophobic interactions.[4,5] The primary function of HSA lies in the maintenance of colloid osmotic pressure within blood vessels. HSA also acts as a carrier for transporting numerous hydrophobic molecules, *e.g.*, steroid hormones, bilirubin, and fatty acids. Due to these properties, HSA is used clinically to treat severe hypoalbuminemia or traumatic shock.[6]

Prulifloxacin (PUFX), 1,6-fluoro-1-methyl-7-[4-(5-methyl-2-oxo-1,3-dioxolen-4-yl)methy-1-piperazinyl]-4-oxo-4*H*-[1,3]thiaceto[3,2-*a*]quinoline-3-carboxylic acid, is a new type of oral antibiotic. It is a new thiazeto-quinolone antibacterial agent prodrug of the quinolone carboxylic acid ulifloxacin, characterized by potent, and broad-spectrum antibacterial activity. It is active against both gram-positive and gram-negative bacteria and several anaerobic and atypical bacteria associated with chronic bronchitis and urinary tract infections.[7,8] PUFX contains a quinolone skeleton with a four-member ring in the 1, 2 position including a sulfur atom to increase antibacterial activity and an anoxodioxolenylmethyl group in the 7-piperazine ring to improve oral absorption. Determination of the active metabolite of prulifloxacin in human plasma using HPLC was reported.[9]

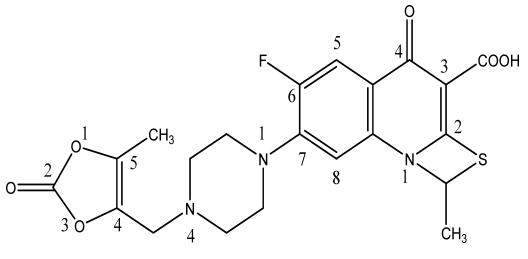


Fig. 1. The Structure of Prulifloxacin

In this paper, we report our studies on the interaction of PUFX with HSA using fluorescence spectrometry. Synchronous fluorescence measurement was employed to probe conformational changes induced by PUFX. Binding parameters were calculated according to fluorescence data, and the binding mode is discussed based on thermodynamic analysis. The precise location of PUFX on HSA was identified in competitive binding experiments and further calculated based on fluorescence resonance energy transfer (FRET).

## Experimental

**Apparatus and Reagents** An FP-6500 fluorescence spectrometer (Jasco, Japan) was used to record the fluorescence spectra. Absorption spectra were recorded on a TU1901 UV/Vis Spectrophotometer (PGeneral, Beijing, China). The pH values of Britton–Robinson (B-R) buffer solutions were measured with a PHS-23 meter (Shanghai Secondly Analytical Instruments, P. R. China).

PUFX solution ($1.0\times10^{-4}$ mol/l) (99.0% purity) was prepared by dissolving PUFX 0.0461 g (461.46 Da, Shanghai Modern Pharmaceutical, Shanghai, P. R. China) in 1000 ml of deionized water. HSA ($1.0\times10^{-4}$ mol/l) was prepared by dissolving 3.3250 g of HSA (66500 Da, Shanghai Wenhao Biochemistry Tech., Shanghai, P. R. China) in 500 ml of water. The solutions were stored at approximately 4 °C. B-R buffer solutions (pH=7.24) were prepared by combining a mixed acid (composed of 0.04 mol/l of $H_3PO_4$, HAc, and $H_3BO_3$) with 0.2 mol/l of NaOH in equal proportions. The buffer solutions were prepared to adjust the acidity of the system. NaCl (0.2 mol/l) was prepared to adjust the ionic strength of the HSA-PUFX solution so as to investigate the effects of electrolytes on binding.

Double-distilled, deionized water was used for the preparation of some solutions. All other chemicals were of analytical grade.

**General Procedure** B-R buffer 1.00 ml, $1.0\times10^{-4}$ mol/l HSA 1.00 ml and an appropriate amount of PUFX were added successively to a 10-ml volumetric flask. The mixture was diluted to an appropriate volume with water and mixed thoroughly by shaking.

The fluorescence spectra of the system were recorded at 285—450 nm. The excitation bandwidth was 5 nm and emission bandwidth was 10 nm, using a 1-cm quartz cell.

* To whom correspondence should be addressed. e-mail: ziyanqin@163.com

© 2010 Pharmaceutical Society of Japan

## Results and Discussion

**Fluorescence Quenching Spectra and Quenching Mechanism of HSA by PUFX** Figure 2 shows that the addition of PUFX caused a dramatic change in the emission spectra. The fluorescence intensity decreased gradually with the increasing concentration of PUFX, and higher concentrations led to more efficient quenching of the protein fluorescence. Such strong quenching clearly indicated the binding of PUFX with HSA. The change in the microenvironment around tryptophan was also confirmed by a red shift in the maximum emission wavelength from 336 to 348 nm, which indicated that the binding of PUFX to HSA quenches the intrinsic fluorescence of the single tryptophan in HSA (Trp-214), and affects the conformation of the protein. Quenching of HSA by PUFX indicated that the antibiotic reached sub domain IIA, where Trp-214 is located.[10] To clarify the fluorescence quenching mechanism induced by HSA, the Stern–Volmer equation Eq. 1 was utilized to process the data.[11]

$$F_0/F=1+K_q\tau_0[Q]=1+K_{SV}[Q]$$

This equation is transformed to:

$$(F_0-F)/F=K_{SV}[Q] \quad (1)$$

where $F_0$ and $F$ represent the fluorescence intensities of HSA in the absence and presence of the quencher (PUFX); [$Q$] is the concentration of the quencher; $K_{SV}$ is the dynamic quenching constant, which is equal to $K_q\times\tau_0$; $K_q$ is the bimolecular quenching rate constant; and $\tau_0$ is the average lifetime of the molecule without quencher. To confirm the quenching mechanism, the procedure of fluorescence quenching was first assumed to be dynamic quenching. According to Eq. 1, the curve of $F_0/F$ *versus* [$Q$] was plotted in Fig. 3. The Stern–Volmer curve was linear when the concentration of PUFX ranged from 1.0 to $2.5\times10^{-5}$ mol/l at 288, 298, and 308 K (see the inset in Fig. 3b). All the plots show a good linear relationship. It is known that linear Stern–Volmer plots represent a single quenching mechanism, either static (the formation of a complex between quencher and fluorophore) or dynamic (a collisional process).[12] In a static quenching process, generally a linear Stern–Volmer plot indicates either only one drug-binding site existing in the proximity of a fluorophore or more than one binding site all equally accessible to quenchers.[13,14] In a dynamic quenching process, the bimolecular quenching constant $K_{SV}$ is expected to increase with rising temperature because it is closely related to diffusions or diffusion coefficients. In addition, the Stern–Volmer slope is expected to depend on the concentration of the donor (HSA) in a static quenching process, whereas the slope is independent of the concentration of donor in a dynamic process. Linear fittings of the experimental data to Eq. 1 afforded the $K_{SV}$ and $k_q$ values listed in Table 1 (Fig. 3b). Table 1 shows that $K_{SV}$ increases with rising temperature. This indicates that the fluorescence quenching of HSA by PUFX occurs a dynamic quenching mechanism. Yet the value for $K_q$ in Table 1 stemmed from $K_q=K_{SV}/\tau_0$, where the value of $\tau_0$ for biopolymers is generally $10^{-8}$/s,[15] is of the magnitude of $10^{12}$ l/mol·s. This is greater than the maximum diffusion collision quenching rate constant ($2.0\times10^{10}$ l/mol·s) for a variety of quenchers with biopolymers. Therefore it suggested that the fluorescence quenching process of HSA may be mainly governed by a static quenching mechanism arising from a system formation rather than a dynamic quenching mechanism.[16]

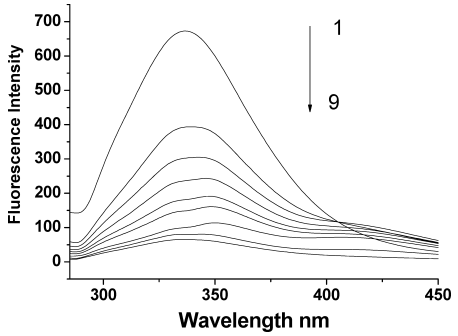


Fig. 2. Fluorescence Quenching of HSA in the Presence of PUFX, $\lambda_{ex}$=281 nm, $C_{HSA}=1.0\times10^{-5}$ mol/l, $C_{PUFX}$=0.0 (1), 1.0 (2), 1.5 (3), 2.0 (4), 2.5 (5), 3.0 (6), 3.5 (7), 4.0 (8), and 4.5 (9)$\times10^{-5}$ mol/l, Respectively, $T$=288 K, pH=7.24

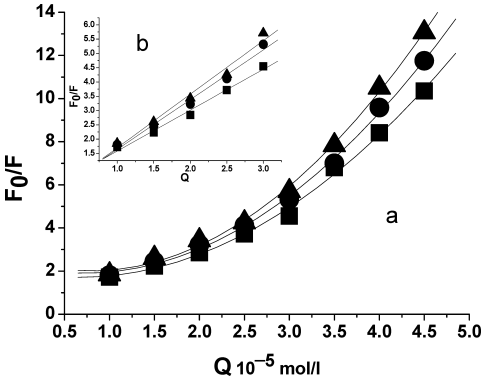


Fig. 3. (a) Plots of $F_0/F$ for HSA against [$Q$] of PUFX Ranging from 1.0 to $4.5\times10^{-5}$ mol/l at Different Temperatures ((■), 288 K; (●), 298 K; (▲), 308 K), $\lambda_{ex}$=281 nm, $\lambda_{em}$=337 nm, $C_{HSA}=1.0\times10^{-5}$ mol/l and (b) Straight Lines in the Inset Are Plots of $F_0/F$ for HSA against [$Q$] of PUFX Ranging from 1.0 to $2.5\times10^{-5}$ mol/l, pH=7.24

Table 1. Stern–Volmer Quenching Constants for HSA–PUFX System at Different Temperatures

| $T$ (K) | $K_{SV}$ ($\times10^5$ l/mol) | $R$ | $K_q$ ($\times10^{13}$ l/mol·s) |
|---|---|---|---|
| 288 | 1.44±0.04 | 0.994 | 1.44±0.04 |
| 298 | 1.80±0.10 | 0.992 | 1.80±0.10 |
| 308 | 1.91±0.05 | 0.990 | 1.91±0.05 |

Each data point represents the arithmetic mean±S.D. of three independent experiments.

In many cases, fluorophores can be quenched by both collision and complex formation with the same quencher. Consequently, the Stern–Volmer plot will exhibit an upward curve, being concave toward the $y$-axis at higher [$Q$] values (Fig. 3a). Accordingly, $F_0/F$ is related to [$Q$] by the following modified form Eq. 2 of the Stern–Volmer equation[17]:

$$F_0/F=(1+K_D[Q])(1+K_S[Q])=1+(K_D+K_S)[Q]+K_Dk_S[Q]^2 \quad (2)$$

where $K_D$ and $K_S$ are the dynamic and static quenching constants, respectively. It is second order in [$Q$] and thus leads to upward curving plots of $F_0/F$ *versus* [$Q$] at higher [$Q$] arising from a combined quenching (both dynamic and static) process.

**Binding Constant and Binding Site** In a static quenching process, when small molecules are bound independently to a set of equivalent sites on a macromolecule, the equilibrium between free and bound molecules was given by Eq. 3[18,19]:

$$\log(F_0-F)/F=\log K_b+n\log[Q] \quad (3)$$

where $K_b$ is the binding constant and $n$ is the number of binding sites. For the PUFX–HSA system in the lower concentration range, $K_b$ and $n$ at different temperatures can be derived from the intercept and slope of plots of $\log(F_0-F)/F$ *versus* $\log[Q]$ based on Eq. 3 and presented in Table 2. Linear regression equations Eqs. 4—6 at 288, 298, and 308 K are expressed as follows:

$$\log(F_0-F)/F=(8.3057\pm0.2102)+(1.70\pm0.04)\log[Q] \quad (4)$$

$$\log(F_0-F)/F=(8.4364\pm0.0789)+(1.71\pm0.01)\log[Q] \quad (5)$$

$$\log(F_0-F)/F=(8.920\pm0.1359)+(1.76\pm0.03)\log[Q] \quad (6)$$

In which each data point represents the arithmetic mean± S.D. of three independent experiments. The values for $K_b$ (Table 2) show that there exists a strong interaction between PUFX and HSA and a complex formation of PUFX with HSA. Furthermore, it can be inferred from the values of $n$ that there is an independent class of binding sites on HSA for PUFX. Otherwise, it appears that the binding constants and the number of binding sites increase with higher temperature.[20,21] This may be because the capacity of PUFX binding to HSA is enhanced with increasing temperature.

**Thermodynamic Parameters and Binding Force between PUFX and HSA** The intermolecular forces contributing to biomolecule interactions with drugs may include hydrogen bonds, Van der Waals interactions, electrostatic interactions, hydrophobic force, *etc.*[22] The thermodynamic parameters for binding interactions will provide strong evidence for the presence of binding forces. If an enthalpy change ($\Delta H^0$) does not vary significantly with temperature, its value and that for an entropy change ($\Delta S^0$) can be determined by the van't Hoff equation:

$$\ln K=-\Delta H^0/RT+\Delta S^0/R \quad (7)$$

Consequently, a free energy change ($\Delta G^0$) for a binding interaction at different temperatures can be evaluated:

$$\Delta G^0=-RT\ln K \quad (8)$$

where $K$ is the binding constant and $R$ the gas constant. The values of $\Delta G^0$, $\Delta H^0$, and $\Delta S^0$ for PUFX binding to HSA are listed in Table 2. A negative value of $\Delta G^0$ reveals that the binding is a spontaneous process. The positive entropy change arises from water molecules arranged more randomly around HSA and the drug, caused by hydrophobic interactions between HSA and drug molecules. The large negative $\Delta H^0$ value probably mainly came from electrostatic interactions. The major contribution to $\Delta G^0$ resulting from the $\Delta H^0$ term rather than from $\Delta S^0$ meant that the binding process was driven by enthalpy and the hydrogen bond was most likely to be the predominant force in the binding process.[23]

**Conformational Changes Investigated by Synchronous Fluorescence** Synchronous fluorescence is a useful tool to investigate the microenvironments around the fluorophore

Table 2. Binding Parameters and Thermodynamic Parameters for HSA–PUFX System at Different Temperatures

| $T$ (K) | $K_b$ ($\times10^8$ l/mol) | $n$ | $R$ | $\Delta G^0$ (kJ/mol) | $\Delta H^0$ (kJ/mol) | $\Delta S^0$ (J/mol·K) |
|---|---|---|---|---|---|---|
| 288 | 2.08±1.04 | 1.70±0.04 | 0.992 | −45.9 | −45.5 | 314 |
| 298 | 2.74±0.50 | 1.71±0.01 | 0.994 | −48.2 | −45.5 | 314 |
| 308 | 4.98±1.61 | 1.76±0.03 | 0.994 | −51.3 | −45.5 | 314 |

Each data point represents the arithmetic mean±S.D. of three independent experiments.

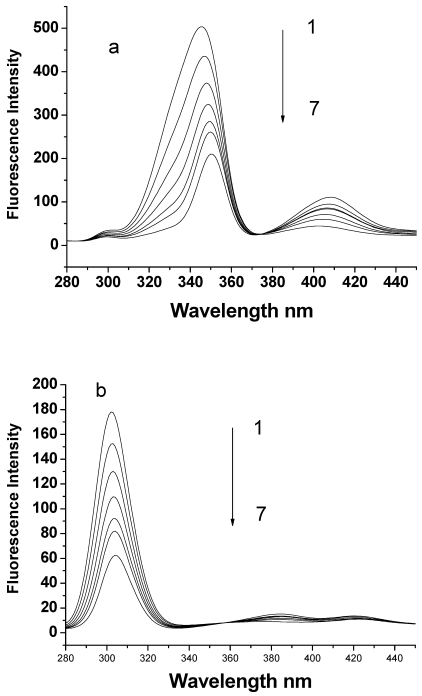


Fig. 4. Synchronous Fluorescence Spectra of HSA with $\Delta\lambda=60$ nm (a) and $\Delta\lambda=15$ nm (b) in the Presence of Increasing Amount of PUFX. $C_{HSA}=1.0\times10^{-5}$ mol/l, $C_{PUFX}=1.0$ (1), 1.5 (2), 2.0 (3), 2.5 (4), 3.0 (5), 3.5 (6), and 4.0 (7)$\times10^{-5}$ mol/l, $T=288$ K, pH=7.24

functional groups. It is well known that the fluorescence of HSA arises from the tyrosine, tryptophan, and phenylalanine residues. The fluorescence of HSA with $\Delta\lambda$ ($\Delta\lambda=\lambda_{emission}-\lambda_{exitation}$) of 60 and 15 nm are characteristic of tryptophan and tyrosine, respectively.[24] The effects of PUFX on synchronous fluorescence spectra are shown in Fig. 4. The synchronous spectra of PUFX were scanned at $\Delta\lambda=60$ nm (Fig. 4a) and $\Delta\lambda=15$ nm (Fig. 4b). It can be seen that the fluorescence spectra of tyrosine (Fig. 4b) was weak and the addition of PUFX resulted in a decrease in intensity and no shift in the maximum emission wavelength ($\lambda_{max}$). The fluorescence of tryptophan (Fig. 4a) was strong, and with the addition of PUFX the fluorescence intensity decreased and the $\lambda_{max}$ shifted from about 345 to 350 nm. It was reported[25] that the maximum emission wavelength at 330—332 nm indicates that the tryptophan residues are located in an apolar region, meaning that they are buried in a hydrophobic cavity; and the $\lambda_{max}$ at 350—352 nm shows tryptophan residues are exposed to water, *i.e.*, the hydrophobic cavity in HSA is disagglomerated and the structure of HSA is looser. In the case of tyrosine, quenching of its fluorescence in the presence of PUFX

indicates that most likely fluorescence in this case is due mainly to one nearby Tyr in subdomain IIA. The location of the Tyr-263 residue is in subdomain IIA, close to the binding site and not completely buried inside the protein. The interaction of PUFX with HSA does not significantly affect the conformation of tryptophan and tyrosine residue microregions. Therefore the observed red shift of $\lambda_{max}$ suggests that PUFX bound to a hydrophobic cavity in HSA, and the polarity around tryptophan increased while the hydrophobicity decreased.[26)]

**Energy Transform between PUFX and HSA** To determine the precise location of PUFX in HSA, the efficiency of energy transfer was studied according to the Förster resonance energy transfer theory.[27)] The fluorescence quenching of HSA after binding with PUFX indicates that the transfer of energy between PUFX and HSA has occurred. The efficient ligand–protein interaction gives rise to energy data, from which the distance between two interacting molecules can easily be evaluated. The efficiency of energy transfer $E$ is described by the following equation[28,29)]:

$$E=1-F/F_0=R_0^6/(R_0^6+R^6) \quad (9)$$

where $F_0$ and $F$ are the fluorescence intensity of the donor in the absence and presence of equal amounts of acceptor, respectively; $R$ is the distance between the acceptor and donor; $R_0$ is the critical distance; and the value of $R_0$ is calculated by the following equation:

$$R_0^6=8.8\times10^{-25}K^2N^{-4}\Phi J \quad (10)$$

where $K^2$ is the spatial orientation factor of the dipole, $N$ the refractive index of the medium, $\Phi$ the fluorescence quantum yield of the donor, $J$ the overlap integral of the fluorescence emission spectrum of the donor, and the absorption spectrum of the acceptor. $J$ is given by

$$J=\int_0^\infty F(\lambda)\varepsilon(\lambda)\lambda^4 d\lambda \Big/ \int_0^\infty F(\lambda)d\lambda \quad (11)$$

In this equation $F(\lambda)$ is the fluorescence intensity of the fluorescent donor of wavelength, $\lambda$, $\varepsilon(\lambda)$ is the molar absorption coefficient of the acceptor at wavelength $\lambda$, $\lambda=100$ nm (100 nm means the width of the wavelength range from 286 to 385 nm to calculate the overlapping integral). It was reported earlier that $K^2=2/3$, $N=1.336$, and $\Phi=0.118$ for HSA.[30)] Figure 5 shows the overlap of the UV absorbance spectrum of PUFX with the fluorescence spectrum of HSA. From the above relationships, the values for $J$, $R_0$, and $R$ are: $J=(9.439\pm1.147)\times10^{-17}$ cm$^3\cdot$l/mol, $R_0=(1.13\pm0.03)$ nm, and $R=(1.19\pm0.02)$ nm for HSA. Each data point represents the arithmetic mean±S.D. of three independent experiments. The distance $R<8$ nm between donor and acceptor indicates that the energy transfer from HSA to PUFX occurred with high probability. Furthermore, the $R$ value of 1.19 nm for HSA, respectively, are larger than 1.13 nm for $R_0$ of HSA in this study, which also show that PUFX could strongly quench the intrinsic fluorescence of HSA by nonradiative energy transfer and static quenching.[31)] This obeys the conditions of the Förster energy transfer theory.

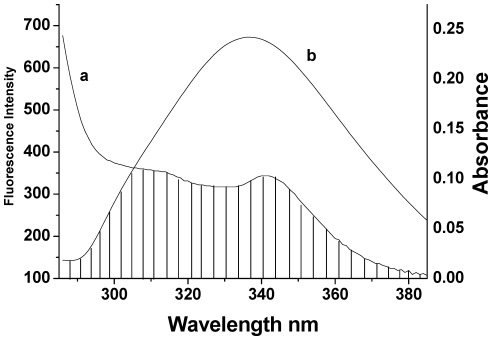


Fig. 5. The Overlap of the UV Absorption Spectrum of PUFX (a) with the Fluorescence Emission Spectrum of HSA (b) when the Molar Ratio of PUFX and HSA Ratio is 1 : 1, $C_{HSA}=C_{PUFX}=1.0\times10^{-5}$ mol/l, $T=288$ K, pH=7.24.

## Conclusion

The interaction between PUFX and HSA was studied under simulated physiologic conditions using fluorescence spectrometry. The apparent binding constant $K_b$ values between PUFX and HSA at different temperatures were obtained, indicating a strong binding affinity. The distance $R<8$ nm between donor and acceptor indicated that the energy transfer from HSA to PUFX occurred with high probability. The determinations performed here may provide an approach to evaluate the effects of chemicals on target proteins and the molecular mechanism of antibiotics. The results obtained are of biological significance because albumin generally serves as a carrier molecule for many drugs in pharmacology and clinical medicine.

**References**

1) Nanda R. K., Sarkar N., Banerjee R., *J. Photochem. Photobiol. A*, **192**, 152—158 (2007).
2) He Y., Wang Y. W., Tang L. F., Liu H., Chen W., Zheng Z. L., Zou G. L., *J. Fluoresc.*, **18**, 433—442 (2008).
3) Petitpas I., Bhattacharya A. A., Twine S., East M., Curry S., *J. Biol. Chem.*, **276**, 22804—22809 (2001).
4) He X. M., Carter D. C., *Nature* (London), **358**, 209—215 (1992).
5) Dockal M., Carter D. C., Ruker F., *J. Biol. Chem.*, **275**, 3042—3050 (2000).
6) Peters T., "All About Albumin: Biochemistry, Genetics and Medical Applications," Chapter 6, Academic Press, San Diego, CA, 1995, pp. 251—284.
7) Imada T., Miyazaki S., Nishida M., Yamaguchi K., Goto S., *Antimicrob. Agents Chemother.*, **36**, 573—579 (1992).
8) Matera M. G., *Pulm. Pharmacol. Ther.*, **19**, 20—29 (2006).
9) Wen J., Zhu Z. Y., Hong Z. Y., Wu Y. W., Fei Y., Lin M., Fan G. R., Wu Y. T., *Chromatographia*, **66**, 37—41 (2007).
10) Li J. H., Liu X. Y., Ren C. L., Li J. Z., Sheng F. L., Hu Z. D., *J. Photochem. Photobiol. B*, **94**, 158—163 (2009).
11) Lakowicz J. R., "Principles of Fluorescence Spectroscopy," Chapter 10, Plenum Press, New York, 1983, pp. 303—339.
12) Eftink M. R., Ghiron C. A., *J. Phys. Chem.*, **80**, 486—493 (1976).
13) Zhao H. W., Ge M., Zhang Z. X., Wang W. F., Wu G. Z., *Spectrochim. Acta Part A*, **65**, 811—817 (2006).
14) Tang J. H., Qi S. D., Chen X. G., *J. Mol. Struct.*, **779**, 87—95 (2005).
15) Lakowicz J. R., Weber G., *Biochemistry*, **12**, 4161—4170 (1973).
16) Ware W. R., *J. Phys. Chem.*, **66**, 455—458 (1962).
17) He Y., Wang Y. W., Tang L. F., Liu H., Chen W., Zheng Z. L., Zou G. L., *J. Agric. Food Chem.*, **18**, 433—442 (2008).
18) Feng X. Z., Lin Z., Yang L. J., Wang C., Bai C. L., *Talanta*, **47**, 1223—1229 (1998).
19) Jiang M., Xie M. X., Liu Y., Li X. Y., Chen X., *J. Mol. Struct.*, **692**, 71—80 (2004).
20) Kandagal P. B., Ashoka S., Seetharamappa J., Shaikh S. M. T., Jadegoud Y., Ijare O. B., *J. Pharm. Biomed.*, **41**, 393—399 (2006).
21) Wei Y. L., Li J. Q., Dong C., Shuang S., Liu D. S., Huie C. W., *Talanta*,

**70**, 377—382 (2006).
22) Leckband D., *Annu. Rev. Biophys. Biomol. Struct.*, **29**, 1—26 (2000).
23) Ross P. D., Subramanian S., *Biochemistry*, **20**, 3096—3102 (1981).
24) Li D. J, Zhu J. F., Jin J., *J. Photochem. Photobiol. A*, **189**, 114—120 (2007).
25) Abou-Zied O. K., Al-Shihi O. I. K., *J. Am. Chem. Soc.*, **130**, 10793—10801 (2008).
26) Zhu J. F., Li D. J., Jin J., Wu L. M., *Spectrochim. Acta Part A*, **68**, 354—359 (2007).
27) Förster T., "Modern Quantum Chemistry," Vol. 3, ed. by Sinaoglu O., Academic Press, New York, 1965.
28) Kenworthy A. K., *Methods*, **24**, 289—296 (2001).
29) Jin J., Zhang X., *J. Lumin.*, **128**, 81—86 (2008).
30) Bertucci C., Domenici E., *Curr. Med. Chem.*, **9**, 1463—1481 (2002).
31) Valeur B., Brochon J. C., "New Trends in Fluorescence Spectroscopy," 6th ed., Springer Press, Berlin, 1999.